The relative contributions of complexation, dispersing, and adsorption of tannic acid to the dissolution of copper oxide nanoparticles

Tan, C.; Liu, Y.; He, Y.; Luo, W.; Zhang, R.; Vijver, M.G.; Peijnenburg, W.J.G.M.

Citation

Tan, C., Liu, Y., He, Y., Luo, W., Zhang, R., Vijver, M. G., & Peijnenburg, W. J. G. M. (2021). The relative contributions of complexation, dispersing, and adsorption of tannic acid to the dissolution of copper oxide nanoparticles. *Water, Air And Soil Pollution*, *232*. doi:10.1007/s11270-021-05322-w

Water Air Soil Pollut (2021) 232: 359
https://doi.org/10.1007/s11270-021-05322-w

The Relative Contributions of Complexation, Dispersing, and Adsorption of Tannic Acid to the Dissolution of Copper Oxide Nanoparticles

Cong Tan · Yang Liu · Ying He · Wenhao Luo · Ruicai Zhang ·
Martina G. Vijver · Willie J. G. M. Peijnenburg

Received: 7 May 2021 / Accepted: 18 August 2021

Abstract Copper oxide nanoparticles (CuO NPs) are one of the most widely used materials owing to their excellent properties such as thermal and photochemical stability, superconductivity, and high electrochemical activity. Once they enter the environment, Cu^{2+} may be released in water, which alters the behavior and toxicity of CuO NPs. The present study thus investigated the dissolution of CuO NPs (40 nm) in the presence of tannic acid (TA), a model chemical of dissolved organic matter. The adsorption of TA decreased the hydrodynamic diameter of CuO NPs and increased the zeta potential of the suspension. Although the adsorption of TA on particle surface improved the dispersion of CuO NPs, their dissolution extents were all reduced at TA concentration up to 55.4 mg C L^{-1}. At pH 5, the contributions of TA complexed Cu to the overall dissolution increased up to 37.8% as a function of TA concentrations. All the findings shown above approved that the strong adsorption of TA played a dominant role in preventing the dissolution of CuO NPs.

Keywords Copper oxide nanoparticles · Tannic acid · Dissolution · Complexation · Dispersing · Adsorption

1 Introduction

With the booming of nanotechnology, more and more metal-based NPs (MNPs) have been applied to improve the life quality and work efficiency (Suttiponparnit et al., 2011). However, new concerns are also raised upon the risks of MNPs to organisms or human beings. The MNPs may undergo various transformations including dissolution, aggregation, and reactions with (bio)macromolecules once entering into the environment. It has been confirmed that metal ions released from MNPs played an important role in their harmful impacts on organisms (Joonas et al., 2019). To better control the risks of MNPs during the application, it is essential to accurately characterize the dissolution of MNPs in different scenarios.

It should be noted that when discharged into the environment, MNPs are involved in various

---

Supplementary Information The online version contains supplementary material available at https://doi.org/10.1007/s11270-021-05322-w.

C. Tan · Y. Liu (✉) · Y. He · W. Luo · R. Zhang
Yunnan Key Laboratory of Soil Carbon Sequestration
and Pollution Control, Faculty of Environmental Science
and Engineering, Kunming University of Science
and Technology, Kunming 650500, China
e-mail: minipig6@163.com

M. G. Vijver · W. J. G. M. Peijnenburg
Institute of Environmental Sciences (CML), Leiden
University, Leiden 2300 RA, the Netherlands

W. J. G. M. Peijnenburg
Center for Safety of Substances and Products, National
Institute of Public Health and the Environment (RIVM),
Bilthoven 3720 BA, the Netherlands

processes, which may inhibit or promote the release of metal ions. For example, MNPs may react with H^+ in aqueous medium, leading to more metal ions release (Liu et al., 2020a; Wang et al., 2016). Meanwhile, the ubiquitous dissolved organic matter (DOM) can be adsorbed onto MNPs and hinder MNPs dissolution. However, DOM may also serve as a dispersing agent (Liu et al., 2020b) for MNPs, or complex with the released metal ions, which are beneficial for the MNPs dissolution. Therefore, the apparent MNPs dissolution is a balance of different processes. How to extract the dominant processes and quantify their contributions to the apparent metal ion release should be the very first step in predicting MNPs behavior and evaluating their risks.

To better understand MNPs behavior in the aqueous phase, the dissolution of CuO NPs was investigated in the presence of tannic acid (TA). CuO NPs were selected as a representative MNPs, because they have gained special interests among various MNPs possibly owing to their high efficiency as nanofluids, nanofertilizer, sensors, antimicrobial applications, catalysis, superconductors energy storage systems, and anticancer agent (Renuga et al., 2020). TA is a natural polyphenolic compound, commonly found in natural environmental media (Chang & Juang, 2004). It has been widely used as a substitute of DOM. The hypotheses raised in this study were thus as follows: (1) the adsorbed TA on the particle surface can disperse CuO NPs; (2) the dissolution of CuO NPs can be increased by TA in the solution.

2 Materials and Methods

2.1 Materials and Characterization

Copper oxide nanoparticles (CuO NPs, nano-spheres, purity 99.5%) in a nominal particle size of 40 nm were purchased from the Aladdin Reagent Company (Shanghai, China). Tannic acid (TA, purity 99.8%) was purchased from the Jicang Company (Tianjin, China). $Cu(NO_3)_2 \cdot 2.5H_2O$ (purity 98.0%) for preparing Cu^{2+} solutions and $NaNO_3$ (purity 99.0%) for preparing the background solution (0.1 M) were both purchased from the Alfa Aesar Company (Tianjin, China).

The actual Cu concentrations in the solution were determined by a flame atomic absorption spectroscopy (FAAS, Hitachi, Japan) after acid digestion, and the actual concentrations of TA were determined by a total organic carbon analyzer (Vario TOC select, Elementar, Germany). The primary morphology and particle size of CuO NPs before and after spiking TA were characterized by a transmission electron microscope (TEM, Tecnai G^2 TF30, FEI Company, Netherlands). The distribution of hydrodynamic diameter and the zeta potential of CuO NPs in the background solution and in the spiked TA solutions were measured by dynamic light scattering (DLS) on a Zeta PALS instrument (Brook Haven, USA). The surface properties of CuO NPs before and after the TA addition were further studied by Fourier transform infrared spectrometer (FTIR, NICOLET iN10 MX, Thermo Scientific, USA).

2.2 Adsorption Experiments

Batch adsorption experiments were conducted to quantitatively analyze the adsorption capacity, equilibrium time, and adsorption rate of TA on CuO NPs. The TA stock solution (100 mg C L^{-1}) was diluted to 0, 5, 10, 25, and 50 mg C L^{-1} with the background solution of $NaNO_3$ (purity 99.0%, 0.1 M). The pH values of the spiked TA solutions were kept at around 5 using either NaOH (0.1 M) or HNO_3 (0.01 M). Then different amounts of CuO NPs were added to TA solutions to reach 0, 25, 50, and 100 mg L^{-1}. After sonication, the vials were sealed with foil to prevent TA decomposition in light, and incubated on a shaker at 25 ℃ (120 rpm) for 120 h to mimic the water flow disturbance. At 2, 4, 8, 10, 24, 34, 48, 72, 96, and 120 h, an aliquot of liquid was collected and centrifuged at 3500 g for 10 min. The TOC contents in the supernatant were then measured using the TOC analyzer. The difference of TOC between the solutions with and without CuO NPs was attributed to TA adsorbed on the CuO NPs. TA concentrations of 17.5, 30, and 40 mg C L^{-1} were added to CuO NPs to measure the adsorption capacity at 120 h. All treatments were repeated twice.

2.3 Dissolution Experiments and Quantification of Dissolved Cu

To detect the dissolved Cu in TA-CuO NPs systems, the dissolution kinetics experiments were also conducted. In the dissolution test, the CuO NPs were mixed with TA in the same way as that in the adsorption measurements. Due to the presence of TA and anions (i.e., OH^- and NO_3^-) in the background solution, the Cu^{2+} may quickly form complexes with these binding ligands (Liu et al., 2020a). Thus, the dissolved Cu in solution may include both free ions and the complexes (including organic and inorganic complexes). The free Cu^{2+} in the system was measured by a Cu-ion selective electrode (CUO1503, Van London-pHoenix, USA) at 2, 4, 6, 8, 24, 34, 48, 72, 96, and 120 h. The complexed Cu concentrations were calculated based on the established complexation curves at various TA levels (pH = 5) (Zhao et al., 2017). The amount of inorganic complexes was assessed by the software of Visual MINTEQ 3.0 (Environmental Protection Agency, USA).

2.4 Data Analysis

TA adsorption on CuO NPs and Cu complexation with TA were calculated based on the same formula. TA adsorption calculation was presented here as an example:

$$q_t = \frac{c_b - c_t}{c_{\text{CuO}}} \tag{1}$$

where q_t is the TA concentration on CuO NPs at time t, mg C g^{-1}; c_b is the TA concentration in solution before CuO NPs addition, mg C L^{-1}; c_t is the TA concentration in the supernatant after CuO NPs addition at time t, mg C L^{-1}; and c_{CuO} is the concentration of CuO NPs in the solution, mg L^{-1}.

The TA adsorption kinetics were fitted by a modified pseudo-first-order or second-order model (Pan et al., 2012) in Origin Pro 8 (Origin Lab, USA):

$$\frac{q_t}{q_e} = 1 - e^{-k_1 t} \tag{2}$$

$$\frac{q_t}{q_e} = \frac{k_2 t}{1 + k_2 t} \tag{3}$$

where q_e is TA concentration on CuO NPs at equilibrium, mg C g^{-1}; k_1 (h^{-1}) and k_2 (g•mgC^{-1}•h^{-1}) are the rate constants of the adsorption; and t is the equilibration time, h.

The Langmuir (Eq. 4) and the Freundlich models (Eq. 5) were both used to fit the sorption isotherms (Chu et al., 2019):

$$q_e = \frac{K_L Q^0 c_e}{1 + K_L c_e} \tag{4}$$

$$\log q_e = \log K_F + \frac{1}{n} \log c_e \tag{5}$$

where Q^0 is the maximum amount of the single layer TA molecules adsorbed on CuO NPs, mg C g^{-1}; K_L is the Langmuir adsorption coefficient, L mg C^{-1}; K_F represents the Freundlich adsorption coefficient, (mg C g^{-1})/(mg L^{-1})^n; n is the nonlinearity factor; and c_e is the TA concentration in the supernatant at equilibrium, mg C L^{-1}.

The binding curves describing the relationship between the free Cu^{2+} activities and the complexed Cu were fitted using the formation function model (Benedetti et al., 1995):

$$ML = \frac{KLM_f}{1 + KM_f} \tag{6}$$

where ML is the concentration of the complexed Cu, K is the complexation stability constant, L denotes the concentration of ligand, and M_f is the free Cu^{2+} activity.

3 Results and Discussion

3.1 CuO NPs Dispersion as Affected by TA

In the absence of TA, the CuO NPs were spherical agglomerates (Fig. 1a), and the size of the agglomerates decreased with the addition of TA (Fig. 1b–c); this implied that the potential risks of CuO NPs to environmental living organisms may still exist even after 120 h. Moreover, the CuO NPs seemed to be surrounded by a layer of light colored TA especially under the exposure of 55.4 mg C L^{-1} TA, which would be discussed in Section 3.2.

The DLS analysis was conducted to further investigate whether the CuO NPs were dispersed by TA. As shown in Fig. 2, the hydrodynamic sizes of pristine CuO NPs were almost 48 ~ 71 times bigger than their primary particle sizes (40 nm). This indicated

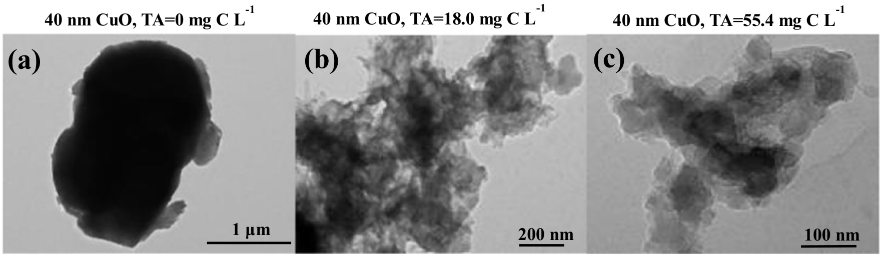

Fig. 1 The TEM images of CuO NPs (37.9 mg L^{-1}, 40 nm) prepared in the background solution (**a**) and in the TA spiked solution (**b**, **c**) after 120 h

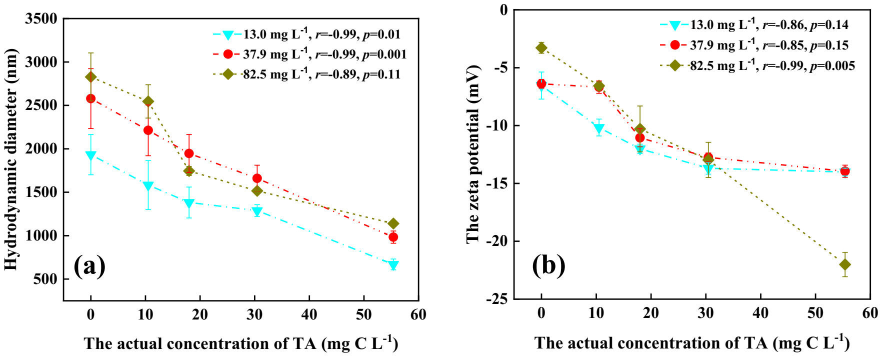

Fig. 2 Dispersion of CuO NPs (13.0, 37.9, and 82.5 mg L^{-1}) at various levels of TA (0, 10.5, 18.0, 30.5, and 55.4 mg C L^{-1}, pH≈5) after 120-h equilibration. The error bars stand for standard errors of the mean. r indicates the Pearson correlation coefficient and p indicates the statistical significance level. **a** represents the relationship between the TA concentration and the hydrodynamic diameter of CuO NPs. **b** represents the relationship between the TA concentration and the zeta potential of CuO NPs

that due to the hydrogen bond and van der Waals force among CuO NPs (Diedrich et al., 2012; Ghosh & Pal, 2007), the aggregation occurred in the present study when particles were put into the solution. A larger hydrodynamic size was observed for high dose of CuO NPs (at TA = 0 in Fig. 2) according to DLS measurement, which is consistent with the decreased repulsion between particles as suggested by zeta potential measurement. After TA addition, the magnitude of the zeta potential increased substantially in an extent much larger than impacts from mass concentration of CuO NPs. For example, at TA concentration of 55.4 mg C L^{-1} and CuO NPs concentration of 82.5 mg L^{-1}, the absolute value of zeta potential was nearly 7 times higher than that of the suspension without TA. Thus, TA addition did disperse CuO NPs, and the dispersed suspension was stable even after 120 h.

3.2 TA Adsorption and Its Relationship with CuO NPs Dispersion

Generally, TA showed strong adsorption on the CuO NPs, e.g., at the mass concentration of 82.5 mg L^{-1}, the amount of TA adsorbed by CuO NPs increased nearly 9 times with the increase of TA concentration (see Fig. 3a). The increasing amount of TA adsorbed on the particle surfaces (Fig. 3c) not only significantly increased the surface charge of CuO NPs but also decreased the hydrodynamic diameter of CuO NPs suspended in the TA spiked solution (Fig. 3b). The details are discussed in Section 3.1. The first hypothesis was thus accepted that the adsorbed TA on the particle surface can serve as a dispersing agent for CuO NPs at various mass concentrations, because the surface charges of CuO NPs at various mass concentrations were all negative no matter whether TA was

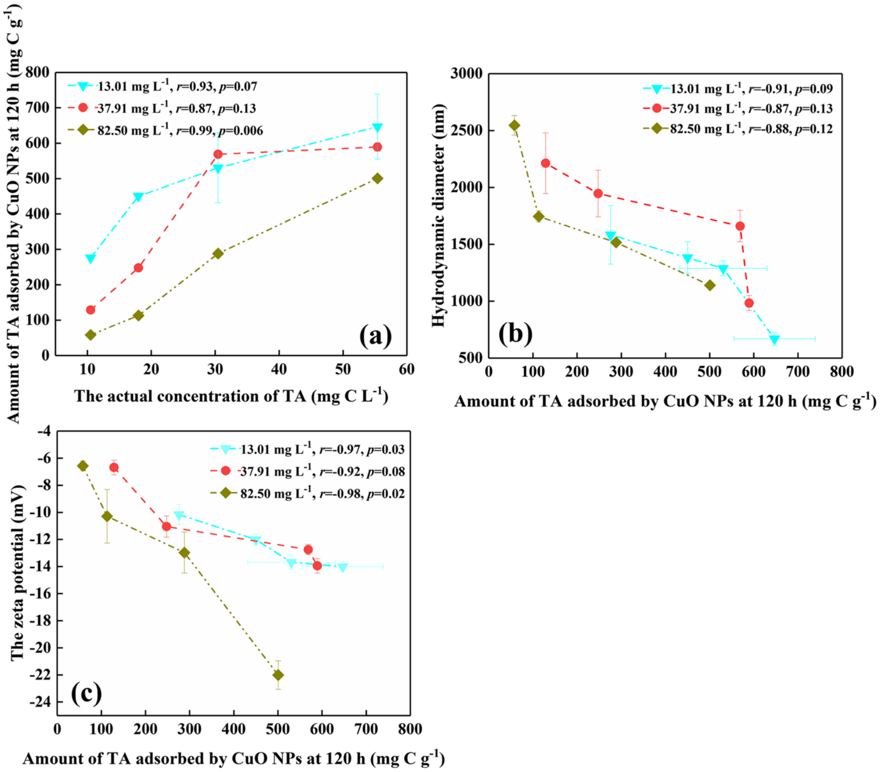

Fig. 3 Adsorption of TA on the particle surface and its relationship with the dispersion of CuO NPs (40 nm) at different concentrations (13.0, 37.9, and 82.5 mg L^{-1}) after 120 h. The data was expressed as the mean ± standard error of the mean. *r* indicates the Pearson correlation coefficient and *p* indicates the statistical significance level

present or not (see Fig. 2b), and TA also showed electronegativity at pH of 5 (Zhao et al., 2017). The better dispersion of CuO NPs in the presence of TA can be possibly due to the intensified electrostatic repulsion or steric hindrance (Jayalath et al., 2018; Liu et al., 2020b) among the TA-coated CuO NPs.

As discussed above, it can be inferred that the adsorption of TA on particle surface may be the result of cation bridging of the released Cu^{2+}, or ligand exchange between phenolic hydroxyl groups on TA (Nebbioso & Piccolo, 2013) and the -OH or $-OH_2^+$ groups on CuO NPs (Gilli & Gilli, 2000) other than the direct electrostatic attraction between TA and CuO NPs. To further understand the dispersing mechanism of TA for CuO NPs, formulas (2) to (5) were used to fit the data. The pseudo-second-order kinetic model represented a better fit than the pseudo-first-order kinetic model especially at higher levels of TA ($R^2_{adj} > 0.75$, Table S1) and CuO NPs ($R^2_{adj} = 0.99$). As shown in Table S2, the Freundlich model performed better than the Langmuir model in assessing relationships between the TA concentration in solid phase and aqueous phase. This further proved that CuO NPs were heterogeneous, leading to uneven distribution of adsorption sites on the particle surface. The orders of fitting parameters, namely K_F (13.01) > K_F (37.91) > K_F (82.50), $1/n$ (13.01) < $1/n$ (37.91) < $1/n$ (82.50), also suggested that adsorption was easy to occur and to get balance faster at lower mass concentrations of CuO NPs, probably due to their better dispersion (Fig. 2). For example, when the concentration of TA was 55.4 mg C L^{-1}, the pseudo-first-order adsorption rate (k_1) decreased by 18 times from 13.0 to 82.5 mg L^{-1} as shown in Table S1.

3.3 Cu Speciation in the TA-CuO NPs System

By comparing the FTIR spectra (Fig. 4) of the bulk TA or CuO NPs with TA in the aqueous phase, the peak intensity of bands was at 1380 cm^{-1} when TA was dissolved in the background solution, indicating

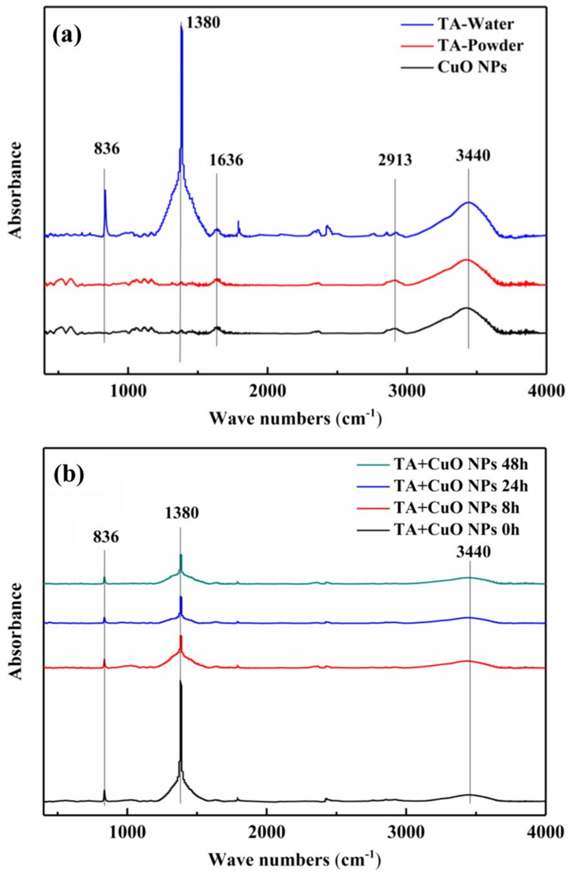

Fig. 4 **a** represents the infrared spectrum of TA in water, TA powder, and CuO NPs. **b** represents the FTIR spectra of TA (30.5 mg C L^{-1}) and CuO NPs (37.9 mg L^{-1}) at different exposure times (0, 8, 24, and 48 h) in the background solution.

the appearance of hydroxyl groups (Givens et al., 2017). It was also found that the peak intensity of hydroxyl groups at 1380 cm^{-1} was getting weaker from 0 to 48 h. The structural changes in TA molecules may be a result of strong interactions of phenolic hydroxyl groups of TA with CuO NPs during the adsorption (Yang et al., 2009), or with the released Cu^{2+} upon the complexation (Zhao et al., 2017). The overall dissolved Cu was the sum of the measured free Cu^{2+} and the complexed Cu. The complexed Cu was calculated through the free Cu^{2+} and the established Cu-TA complexation curves (Figure S1).

In general, under different solid–liquid ratios, CuO NPs kept on dissolving over 120 h (Fig. 5) at a low dissolution rate (Table S3). At a fixed TA concentration, the dissolution rate of CuO NPs increased with particle concentration, e.g., $k_{82.5}$ (0.12 h^{-1}) > $k_{13.0}$ (0.002 h^{-1}) (Table S3). According to the Noyes-Whitney equation (Borm et al., 2006), dissolution rate was positively related to contact area. In the current study, the increased CuO NPs concentration will increase the contact area between the solute and the solution, which consequently accelerated the CuO NPs dissolution. However, the adsorption of TA may thicken the diffusion layer of CuO NPs, which is inversely proportional to the dissolution rate according to the Noyes-Whitney equation. For instance, when the concentration of CuO NPs was 13.0 mg L^{-1}, the concentration of TA absorbed on CuO NPs at equilibrium increased from 265.8 to 474.0 mg C g^{-1}, while the dissolution rate decreased by 3 times (Table S3). Therefore, at the same CuO NPs concentration, the addition of TA decreased the dissolution rate.

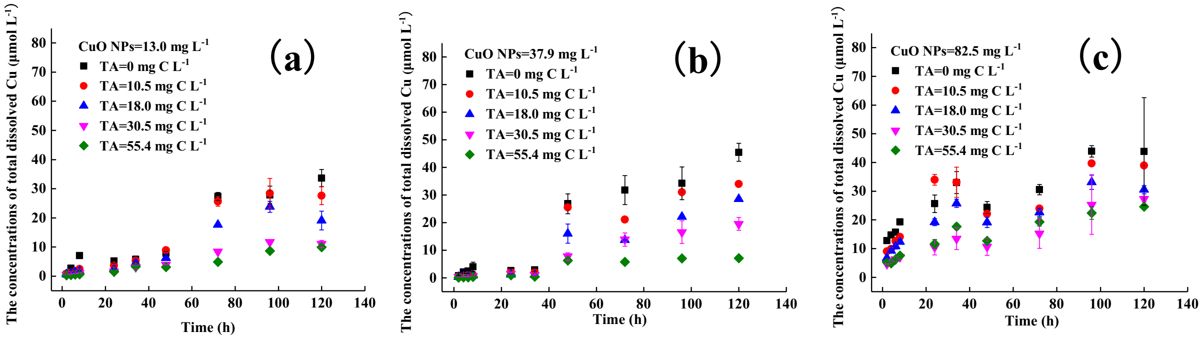

Fig. 5 Dissolution kinetics of CuO NPs (40 nm) at different mass concentrations of 13.0, 37.9, and 82.5 mg L^{-1} and at various levels of TA (0, 10.5, 18.0, 30.5, and 55.4 mg C L^{-1}) within 120 h

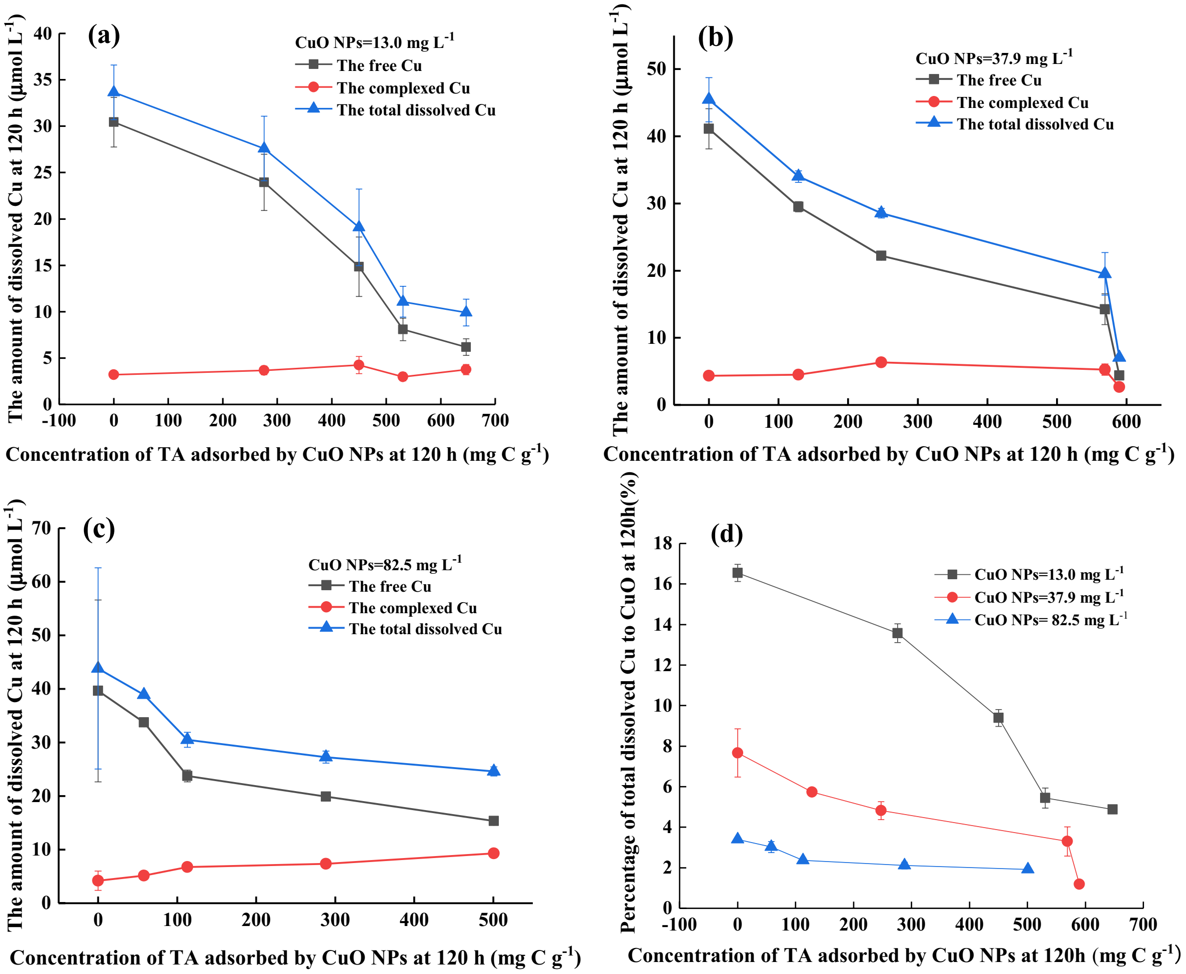

Fig. 6 Dissolution of CuO NPs (40 nm) and Cu speciation in the system with different mass concentrations of 13.0, 37.9, and 82.5 mg L^{-1} and at various levels of TA (0, 10.5, 18.0, 30.5, and 55.4 mg C L^{-1}) after 120 h. The amount of complexed Cu refers to the inorganic complexes calculated by the software of Visual MINTEQ 3.0 when TA = 0 mg C L^{-1}; the amount of complexed Cu refers to the sum of inorganic and organic complexes calculated using the complex titration method when TA > 0 mg C L^{-1}

The speciation analysis was conducted to further understand the influence from TA on the dissolution of CuO NPs. Results showed that the total dissolved Cu and free Cu^{2+} decreased with the solid phase TA concentration for the investigated three CuO NPs concentrations (Fig. 6). Similar result was observed when the overall dissolution was calculated as the percentage of Cu release from CuO NPs at 120 h (Fig. 6d). The above evidences rejected our second hypothesis, and the dissolution extent of CuO NPs was actually reduced by the added TA in the solution. For example, the amount of total dissolved Cu at CuO NPs of 37.9 mg L^{-1} declined more than 84% from TA = 0 to TA = 55.4 mg C L^{-1} (Fig. 6b). Moreover, at a fixed concentration of TA, the percentage of total dissolved Cu to CuO NPs was reduced by the increased concentration of TA (Fig. 6d). The homoaggregation of CuO NPs may be an explanation (Holsapple et al., 2005), which was promoted as more particles were added in the solution (Fig. 2). At a fixed CuO NPs concentration, the increase of TA concentration did not significantly alter the complexed Cu concentration (Fig. 6a–c). The increased addition of TA in the solution mainly raised the TA adsorption on the surface of CuO NPs, while the amount of complexed Cu kept similar at the solution pH of 5. The contributions of complexation to the CuO NPs dissolution would be further discussed in the following section.

3.4 Relative Contributions of TA-Cu Complexation, TA Dispersing, and TA Coating to the Dissolution of CuO NPs as Affected by TA

According to the discussion shown above, the increased adsorption of TA on the particle surface with the increasing TA concentrations did increase the dispersion of 40-nm CuO NPs in the solution. However, the adsorption and dispersion of TA did not promote the dissolution of CuO NPs as expected, which suggested that TA coating played a more intense role than TA dispersing in affecting the dissolution of CuO NPs under the present experimental conditions. The reduced dissolution extent of CuO NPs was thus determined by the sum of the effective areas of CuO NPs exposed to the solution increased by TA dispersing minus the ones decreased by TA coating. With a poor stability, the amount of TA adsorbed by CuO NPs at 82.5 mg L^{-1} after 120 h was always smaller than that at concentrations of 13.0 mg L^{-1} and 37.9 mg L^{-1} across various levels of TA (Fig. 3a). This explained why the decrease of degree of total dissolved Cu (i.e., dispersing-coating) due to TA was the least for CuO NPs at 82.5 mg L^{-1} (Table 1). Afterward, the CuO NPs exposed in the solution also reacted with H^+ or complexed with TA, leading to the solute, i.e., different species of Cu further introduced into the solution. As shown in Table 1, the relative contributions of H^+ (from 90.5 to 22.2%) and complexation reactions (from 13.2 to 37.8%) were only influenced by the added TA content in the solution. At the solution pH value of 5, the contribution of complexation to the dissolution of CuO NPs was less than 50% even at the highest TA concentration of 55.4 mg C L^{-1}. This was in agreement with our previous finding (Zhao et al., 2017) that a lower contribution of complexation to the dissolution of CuO NPs appeared in acid conditions. Percentage of complexation to dissolution was only related to the amount of TA added in the solution, but not influenced by the mass concentration of CuO NPs. The binding affinity of Cu^{2+} to dissolved organic matters was proportional to the ligand concentrations (Liu et al., 2020a; Zhao et al., 2017), thus leading to the upward tendency of percentage of complexation to dissolution and also the increased complexation stability constant (log *K*) from 1.8 to 2.5 (Figure S1) as the TA concentration increased.

4 Conclusions

The influence of TA on the dispersion and dissolution of CuO NPs (40 nm) was investigated for three mass concentrations of 13.0 mg L^{-1}, 37.9 mg L^{-1}, and

Table 1 Relative contributions of H^+, complexation, dispersion, and TA coating to the dissolution of CuO NPs at different mass concentrations after 120-h exposure to various levels of TA

Particle mass (mg L^{-1})	Contributions (%)	TA concentrations (mg C L^{-1})				
		0	10.5	18.0	30.5	55.4
13.0	H^+	90.5	86.8	77.8	73.0	62.2
	Complexation	9.5	13.2	22.2	27.0	37.8
	Dispersing-coating	0	− 18.0	− 43.3	− 67.1	− 70.5
37.9	H^+	90.5	86.8	77.8	73.0	62.2
	Complexation	9.5	13.2	22.2	27.0	37.8
	Dispersing-coating	0	− 25.2	− 37.2	− 57.1	− 84.4
82.5	H^+	90.5	86.8	77.8	73.0	62.3
	Complexation	9.5	13.2	22.2	27.0	37.7
	Dispersing-coating	0	− 11.2	− 30.4	− 37.8	− 43.8

Dispersing indicates the dissolution promoted by the enhanced dispersion or increased surface area exposed to the solution in the presence of TA; -coating indicates the dissolution inhibited by the increased adsorption of TA or decreased surface area exposed to the solution in the presence of TA; the contribution of dispersing-coating indicates the degree of decrease of total dissolved Cu in the presence of TA as compared to that without TA. Percentage of complexation to dissolution refers to the concentration of complexed Cu divided by the total concentration of dissolved Cu in the solution

82.5 mg L^{-1}. Adsorption of TA on the particle surface did play an important role in the improved dispersion of CuO NPs in the aqueous medium by increasing the magnitude of zeta potential and decreasing hydrodynamic sizes (the 1st hypothesis verified). However, the TA dispersing did not dominate the dissolution of CuO NPs. Instead, the wrapping of TA on the particle surface leads to the less free Cu or total Cu dissolved from CuO NPs across different mass concentrations (the 2nd hypothesis rejected). The action of H^+, TA-Cu complexation, TA dispersing, and TA coating all contributed to the dissolution of CuO NPs. Among which, the extent of TA dispersing for the particles was smaller than the extent of TA coating, thus resulting in a bigger magnitude of the decreased dissolution of CuO NPs with increasing levels of TA. The relative contributions of H^+ and TA-Cu complexation to the dissolution of CuO particles were only related to the concentrations of TA in the solution. These findings would further our understandings about behaviors of CuO NPs in the environment, and also be beneficial to risk assessment and control of related products in the near future.

Funding This research was supported by the National Natural Science Foundation of China (41967039); the Yunnan Provincial Ten Thousand Plan (YNWR-QNBJ-2019–065); and the Yunnan Basic Research Plan (202001AT070042).

Data Availability The datasets used or analyzed during the current study are available from the corresponding author on a reasonable request.

Declarations

Competing Interests The authors declare no competing interests.

References

Benedetti, M. F., Milne, C. J., Kinniburgh, D. G., Riemsdijk, W. H. V., & Koopal, L. K. (1995). Metal ion binding to humic substances: Application of the non-ideal competitive adsorption model. *Environmental Science & Technology, 29*, 446–457.

Borm, P., Klaessig, F. C., Landry, T. D., Moudgil, B., Pauluhn, J., Thomas, K., Trottier, R., & Wood, S. (2006). Research strategies for safety evaluation of nanomaterials, part V: Role of dissolution in biological fate and effects of nanoscale particles. *Toxicological Sciences, 90*(1), 23–32.

Chu, G., Zhao, J., Liu, Y., Lang, D., Wu, M., Pan, B., & Steinberg, C. E. W. (2019). The relative importance of different carbon structures in biochars to carbamazepine and bisphenol A sorption. *Journal of Hazardous Materials, 373*, 106–114.

Chang, M. Y., & Juang, R. S. (2004). Adsorption of tannic acid, humic acid, and dyes from water using the composite of chitosan and activated clay. *Journal of Colloid and Interface Science, 278*(1), 18–25.

Diedrich, T., Dybowska, A., Schott, J., Valsami-Jones, E., & Oelkers, E. H. (2012). The dissolution rates of SiO_2 nanoparticles as a function of particle size. *Environmental Science & Technology, 46*(9), 4909–4915.

Gilli, G., & Gilli, P. (2000). Towards an unified hydrogen-bond theory. *Journal of Molecular Structure, 552*(1–3), 1–15.

Givens, B. E., Xu, Z., Fiegel, J., & Grassian, V. H. (2017). Bovine serum albumin adsorption on sio2 and tio2 nanoparticle surfaces at circumneutral and acidic ph: A tale of two nano-bio surface interactions. *Journal of Colloid & Interface Science, 493*, 334–341.

Ghosh, S. K., & Pal, T. (2007). Interparticle coupling effect on the surface plasmon resonance of gold nanoparticles: From theory to applications. *Chemical Reviews, 107*(11), 4797–4862.

Holsapple, M. P., Farland, W. H., Landry, T. D., MonteiroRiviere, N. A., Carter, J. M., Walker, N. J., & Thomas, K. V. (2005). Research strategies for safety evaluation of nonmaterials, part II: Toxicological and safety evaluation of nanomaterials, current challenges and data needs. *Toxicological Sciences, 88*(1), 12–17.

Jayalath, S., Wu, H., Larsen, S. C., & Grassian, V. H. (2018). Surface adsorption of Suwannee River humic acid on TiO2 nanoparticles: A study of pH and particle size. *Langmuir, 34*(9), 3136–3145.

Joonas, E., Aruoja, V., Olli, K., & Kahru, A. (2019). Environmental safety data on CuO and TiO_2 nanoparticles for multiple algal species in natural water: Filling the data gaps for risk assessment. *Science of the Total Environment, 647*, 973–980.

Liu, S., Liu, Y., Pan, B., He, Y., Li, B., Zhou, D., Xiao, Y., Qiu, H., Vijver, M. G., & Peijnenburg, W. J. G. M. (2020). The promoted dissolution of copper oxide nanoparticles by dissolved humic acid: Copper complexation over particle dispersion. *Chemosphere, 245*, 125612.

Liu, Y., Pan, B., Li, H., Lang, D., Zhao, Q., Zhang, D., Wu, M., Steinberg, C., & Xing, B. (2020). Can the properties of engineered nanoparticles be indicative of their functions and effects in plants? *Ecotoxicology and Environmental Safety, 205*, 111128.

Nebbioso, A., & Piccolo, A. (2013). Molecular characterization of dissolved organic matter (DOM): A critical review. *Analytical and Bioanalytical Chemistry, 405*, 109–124.

Pan, B., Wang, P., Wu, M., Li, J., Zhang, D., & Xiao, D. (2012). Sorption kinetics of ofloxacin in soils and mineral particles. *Environmental Pollution, 171*, 185–190.

Renuga, D., Jeyasundari, J., ShakthiAthithan, A. S., & Brightson Arul Jacob, Y. (2020). Synthesis and characterization of copper oxide nanoparticles using Brassica oleracea var italic extract for its antifungal application. *Material Research Express, 7*, 045007.

Suttiponparnit, K., Jiang, J., Sahu, M., Suvachittanont, S., Charinpanitkul, T., & Biswas, P. (2011). Role of surface area, primary particle size, and crystal phase on titanium dioxide nanoparticle dispersion properties. *Nanoscale Research Letters, 6*(1), 27.

Wang, Z., Zhang, L., Zhao, J., & Xing, B. (2016). Environmental processes and toxicity of metallic nanoparticles in aquatic systems as affected by natural organic matter. *Environmental Science Nano, 3*, 240–255.

Yang, K., Lin, D., & Xing, B. (2009). Interactions of humic acid with nanosized inorganic oxides. *Langmuir, 25*, 3571–3576.

Zhao, J., Liu, Y., Pan, B., Gao, G., Liu, Y., Liu, S., Liang, N., Zhou, D., Vijver, M. G., & Peijnenburg, W. J. G. M. (2017). Tannic acid promotes ion release of copper oxide nanoparticles: Impacts from solution pH change and complexation reactions. *Water Research, 127*, 59–67.